ORIGINAL ARTICLE

Repetitive transcranial magnetic stimulation induced modulations of resting state motor connectivity in writer's cramp

R. D. Bharath[a], B. B. Biswal[b], M. V. Bhaskar[a], S. Gohel[b], K. Jhunjhunwala[c], R. Panda[a], L. George[a], A. K. Gupta[a] and P. K. Pal[c]

[a]*Department of Neuroimaging and Interventional Radiology, National Institute of Mental Health and Neurosciences (NIMHANS), Bangalore, Karnataka, India;* [b]*Department of Biomedical Engineering, New Jersey Institute of Technology, Newark, NJ, USA; and* [c]*Department of Neurology, National Institute of Mental Health and Neurosciences (NIMHANS), Bangalore, Karnataka, India*

Keywords:
RSFC, rsfMRI, rTMS, sensory motor network, writer's cramp

Received 5 July 2014
Accepted 17 November 2014

European Journal of Neurology 2015, **22:** 796–805

doi:10.1111/ene.12653

Background and purpose: Writer's cramp (WC) is a focal task-specific dystonia of the hand which is increasingly being accepted as a network disorder. Non-invasive cortical stimulation using repetitive transcranial magnetic stimulation (rTMS) has produced therapeutic benefits in some of these patients. This study aimed to visualize the motor network abnormalities in WC and also its rTMS induced modulations using resting state functional magnetic resonance imaging (rsfMRI).

Methods: Nineteen patients with right-sided WC and 20 matched healthy controls (HCs) were prospectively evaluated. All patients underwent a single session of rTMS and rsfMRI was acquired before (R1) and after (R2) rTMS. Seed-based functional connectivity analysis of several regions in the motor network was performed for HCs, R1 and R2 using SPM8 software. Thresholded ($P < 0.05$, false discovery rate corrected) group level mean correlation maps were used to derive significantly connected region of interest pairs.

Results: Writer's cramp showed a significant reduction in resting state functional connectivity in comparison with HCs involving the left cerebellum, thalamus, globus pallidus, putamen, bilateral supplementary motor area, right medial prefrontal lobe and right post central gyrus. After rTMS there was a significant increase in the contralateral resting state functional connectivity through the left thalamus–right globus pallidus–right thalamus–right prefrontal lobe network loop.

Conclusions: It is concluded that WC is a network disorder with widespread dysfunction much larger than clinically evident and changes induced by rTMS probably act through subcortical and trans-hemispheric unaffected connections. Longitudinal studies with therapeutic rTMS will be required to ascertain whether such information could be used to select patients prior to rTMS therapy.

Introduction

Writer's cramp (WC) is the most common idiopathic task-specific focal hand dystonia, a movement disorder thought to develop in individuals with a genetic susceptibility whilst repetitively performing a highly skilled movement [1,2]. It is characterized by excessive contractions of agonist and antagonist hand and forearm muscles during writing [3]. There are several hypotheses regarding the underlying aetiopathogenesis of WC. One of the popular hypotheses has been related to disturbed surrounding inhibition suggesting an inability to focus appropriate motor neuronal response resulting in tremor as suggested by an earlier transcranial magnetic stimulation (TMS) study

Correspondence: Dr P. K. Pal, Department of Neurology, National Institute of Mental Health and Neurosciences (NIMHANS), Hosur Road, Bangalore 560029, Karnataka, India (tel.: +91 80 26995147; fax: +91 80 26562829; e-mail: pal.pramod@rediffmail.com).
R. D. Bharath and B. B. Biswal contributed equally to this work.

EUROPEAN JOURNAL OF NEUROLOGY

[4]. Another hypothesis is an increase in excitability of motor regions from changes in neurotransmitter and/or receptor function, particularly dopamine [5–7] and GABA [8]. Excessive use of a motor programme could also result in brain plasticity leading to a vicious cycle of motor sensitization and overactivity resulting in tremors. It has been found that therapies promoting reorganization of sensory regions, including constraint-induced movement therapy [9] and proprioceptive training [10], could alleviate the symptoms in WC giving rise to the hypothesis of altered sensory motor integration as the primary cause in WC.

Recent task-based functional magnetic resonance imaging (fMRI) studies have provided valuable insights into the functional correlates of WC, implicating abnormal activities in the cerebellum, dorsal premotor cortex and supplementary motor area (SMA) [11–17] or altered representation of the sensory cortex in some form [17,18] in focal dystonias. Structural studies have shown decreased grey matter volume in the hand area of the left primary sensorimotor cortex, bilateral thalamus and cerebellum in WC patients implicating widespread involvement of the motor system [19]. Earlier diffusion-tensor imaging studies have also supported impaired structural connectivity in the corticospinal tract and thalamus [20] in WC patients. Evidence from the aforementioned imaging studies implicating abnormalities in the sensorimotor cortex, basal ganglia and cerebellum along with various experimental studies [21–23] have supported the hypothesis of WC being a network disorder [24] with pathology being primarily in the motor cortex.

Repetitive transcranial magnetic stimulation (rTMS) protocols applied in a variety of clinical settings in combination with electroencephalography (EEG), positron emission tomography and fMRI have revealed widespread distributed changes in brain activity following rTMS [25,26]. Studies using EEG functional connectivity measures such as coherence have proved that rTMS can alter the strength of connections between cortical regions, and successful rTMS therapy is shown to be related to modulation of the entire network (inter-hemispheric and interregional connections) rather than just a local region [27]. Schneider *et al.* [28] conducted task-based fMRI in conjunction with 5 Hz rTMS on five patients with writers' dystonia and showed induced modulation of the sensorimotor cortex and differential decrease in basal ganglia activation compared with controls. In a similar study by Havrankova *et al.* [29] in four patients low frequency rTMS has been shown to increase task-induced BOLD activation in the bilateral sensorimotor cortex, posterior parietal cortex and the SMA.

One drawback of using task-based fMRI to study focal dystonia is the large inter-subject variance in task activations associated with task performance which may be compromised in WC patients. Resting state fMRI (rsfMRI) is a novel method gaining rapid momentum in its popularity for studying neurological disorders due to its non-dependence on task paradigms, capability of all-inclusive network evaluation and ease of data acquisition. Recent studies evaluating resting state network abnormalities in dystonia patients have reported a disease-induced under-connectivity in the sub-segments of motor networks evaluated [15,30–32]. Most of these studies have focused on the sensorimotor cortex and the premotor cortex based on earlier task-specific fMRI abnormalities. A recent study by Mohammadi *et al.* [33] found additional abnormalities in the default-mode network in WC with increased connectivity of the left putamen.

The goal of the current work was to study the entire motor network in WC using rsfMRI. In addition, our aim was also to understand the whole brain modulations of resting state functional connectivity (RSFC) induced by rTMS which could not be assessed using previous EEG rTMS studies. Our hypothesis was that WC patients will have entire motor network functional connectivity abnormalities and rTMS will alter these abnormalities.

Methodology

Nineteen male patients with WC with a mean age of 35 years (SD ±4.9 years) were prospectively recruited. Twenty age, gender and education matched healthy controls (HCs) with no family history of neurological or psychiatric diseases were recruited as a control group. All subjects were right handed and patients with WC had dystonia only whilst writing. Average age at onset of symptoms was 32.17 years (SD ±5.65) and mean symptom duration was 3.1 years (SD ±0.7). Both the patients and the controls were evaluated in detail by a single movement disorder specialist (PKP) and patients on medications were asked to withhold these drugs for 1 week before the experiment. The demographic details of the patients are included in Table 1. Inclusion criteria for all subjects were a normal MRI study and absence of any brain, spinal or peripheral nerve trauma/surgery. Secondary causes of dystonia were ruled out in all patients by appropriate investigations. None of the patients had a history of botulinum toxin therapy during their lifetime. All patients underwent two sessions of MRI, one prior to the rTMS (R1) and the other immediately after the rTMS (R2). The mean time delay between the rTMS

Table 1 Demographic details of the patients

	Sex	Age	Duration	Medications	Wrist dystonia	Thumb dystonia	Index finger dystonia	Dystonic tremor whilst writing
1	M	21	2	Trihexiphenidyl	Extension	Flexion	No	No
2	M	21	3	Gabapentine/baclofen	Extension	Flexion	Flexion	No
3	M	57	1	Gabapentin/baclofen	Extension	Flexion	No	Yes
4	M	26	4	NIL	Extension	Flexion	No	No
5	M	23	2	Clonazepam	Extension	Flexion	Flexion	No
6	M	40	1	NIL	Extension	Flexion	Flexion	No
7	M	50	2	Trihexiphenidyl/baclofen	Extension and ulnar deviation	Flexion	No	Yes
8	F	40	6	Trihexiphenidyl and clonozepam	Flexion and ulnar deviation	Flexion	No	No
9	M	21	0.5	NIL	Flexion and ulnar deviation	Flexion	No	No
10	M	37	0.5	NIL	Extension and ulnar deviation	Flexion	No	No
11	M	26	3	Trihexiphenidyl/baclofen	Extension	Flexion	Flexion	Yes
12	M	38	0.5	NIL	Flexion with radial deviation	Flexion	Flexion	Yes
13	M	23	3	NIL	Ulnar deviation	Flexion/Extension	No	No
14	M	58	10	NIL	Flexion and ulnar deviation	Flexion	Flexion	No
15	M	53	10	NIL	Flexion and radial deviation	Flexion	No	Yes
16	M	54	3	NIL	Extension with radial deviation	Flexion	Flexion	No
17	M	49	15	Tetrabenazine	Extension and ulnar deviation	Extension	No	No
18	M	49	0.5	NIL	Extension	Flexion	No	Yes
19	M	33	3	Pacitane/baclofen	Flexion with radial deviation	Flexion	No	Yes
20	M	28	1	NIL	Extension	Flexion	Flexion	No

session and R2 was 10 min. HCs were scanned only once and did not undergo an rTMS session. No subject experienced any untoward incident during the procedure. Institute ethics committee approval was obtained for the study. Written informed consent was obtained from each of the participants and the study was approved by the institution review board of the NIMHANS.

Magnetic resonance imaging acquisition parameters

During the data acquisition the subjects were instructed to remain in a relaxed state without engaging in cognitive or motor activity and to keep their eyes closed. rsfMRI images were acquired using a 3 T scanner (Skyra; Siemens, Erlangen, Germany). 185 volumes of spin echo echo-planar images (EPI) were obtained using the following EPI parameters: 36 slices, 4 mm slice thickness in interleaved manner with an FOV of 192 × 192 mm, matrix 64 × 64, repetition time 3000 ms, echo time 35 ms, re-focusing pulse 90°, matrix 256 × 256 × 114, voxel size 3 × 3 × 4 mm. A three-dimensional magnetization-prepared rapid acquisition gradient echo (MPRAGE) sequence for anatomical information (with voxel size 1 × 1 × 1 mm, 192 × 256 matrix) for better registration and overlay of brain activity was also acquired. The acquisition parameters were kept identical for R1 and R2 for WC patients and for HCs.

Repetitive transcranial magnetic stimulation acquisition parameters

A Magstim Super Rapid stimulator (Magstim Co. Ltd, Whitland, UK) with a figure-of-eight coil configuration was used for all patients. Size was recorded from the right first dorsal interosseous at rest by delivering 900 stimuli (90% of resting motor threshold, RMT) at 1 Hz for 15 min. The RMT was calculated by applying single-pulse TMS stimulation using a TMS stimulator attached to an electromyography machine. Motor evoked potential was recorded from the first dorsal interosseous muscle using Ag-AgCl surface electrodes placed over the muscle in a belly tendon arrangement. The RMT determined the lowest intensity that produced motor evoked potentials of >50 μV in at least five out of 10 trials. These were applied tangentially to the scalp with the handle pointing backwards and laterally at an approximate angle of 45° to the mid-sagittal line, and perpendicular to the presumed direction of the central sulcus.

Data analysis

Preprocessing

For each subject, the data processing scheme based on SPM8 software (Functional Imaging Laboratory, Wellcome Trust Centre for Neuroimaging, Institute of Neurology, UCL, London, UK) was implemented.

In the first step, the first five functional images were discarded from each of the subjects' rsfMRI data to allow for signal equilibration. After discarding the first five images, each of the remaining images was registered to mean image to correct for head movements within the scan using the 'realign' tool in SPM8. During the motion correction step, head motions in six directions (x, y, z, roll, pitch and yaw) were recorded. Following realignment each of the functional images was co-registered to MPRAGE images for each of the subjects. After co-registration MPRAGE images were segmented into grey matter, white matter (WM) and cerebrospinal fluid (CSF) and distinct probability maps were derived for each of these segments using the 'new segment' tool in SPM8. During segmentation deformation fields were calculated to transform each of the MPRAGE images into MNI (Montreal Neurological Institute) standard space. For each of the subjects the WM/CSF probability maps were thresholded at $P > 0.99$ to derive binary masks representing WM/CSF. Functional images for each of the subjects were transformed in MNI standard space using the deformation field derived in the new segmentation procedure and downsampled to 3 mm isotropic voxel size to make group comparison feasible. For each of the subjects, WM/CSF masks were used to extract time series from EPI data pertaining to WM and CSF. These time series were extracted using in-house developed MATLAB scripts that used built-in SPM* functions (spm_read_vol.m). Principal component analysis was performed using the PRINCOMP function in MATLAB (R2012b). A total of 34 nuisance time series were used as covariates in the linear regression model to minimize the effects of physiological and motion signals. These included the first five principal components of the WM and CSF time series, six time series describing head motion, six time series describing head motion at previous time points and 12 quadratics of motion time series (Friston 24 model). Following linear regression, the BOLD fMRI data for each of the subjects were spatially smoothed with 6 mm full width at half maximum Gaussian blur and temporally filtered between 0.01 and 0.1 Hz.

Connectivity analysis

In order to study differences in RSFC of the motor network and its subcomponents, seed-based connectivity analysis was performed. A total of 41 seed regions (Table 2) corresponding to the motor network and its sub-cortical components were selected based on earlier studies. For each of the seed regions, a 6 mm sphere was created surrounding the centre voxel coordinated in MNI space and downsampled to 3 mm isotropic voxel size. Average time series were extracted for each of these seed regions of interest (ROIs). Pearson's correlation coefficient was calculated between this average seed time series and between the time series from all the brain voxels to subject level seed-based correlation maps. Each of these seed-based correlation maps was transformed into a Z score using Fisher's $r-Z$ transformation. Voxel-based group level statistics were computed to compare connectivity maps between the control group and WC patients and to derive group level seed-based mean connectivity maps for each of the seed ROIs and for each of the groups.

To study the mean connectivity pattern between all the subcomponents of the motor network, the group level seed-based correlation maps derived in the previous step were used. For each of the seed ROIs, the group level mean correlation map was thresholded ($P < 0.05$, false discovery rate corrected) to derive all the brain voxels that significantly correlated with the seed region. From this thresholded seed-based correlation map, the number of overlapping voxels that passed the statistical threshold and were within 6 mm radius of the target ROI coordinate was calculated. Each of the seed and target ROI pairs that displayed >95% overlapping voxels was considered connected. This procedure was repeated for each of the seed regions and for each of the groups to derive a group level connectivity matrix, which displayed each of the significantly connected ROI pairs for each of the groups. These matrices were displayed using an in-house developed MATLAB program to study topographical changes in connectivity patterns across groups and as an effect of rTMS (Fig. 1).

To study differences in the mean connectivity strength for each of the ROI pairs, Pearson's correlation coefficient was calculated between average time series for each of 820 ROI pairs [$n \times (n - 1)/2$, $n = 41$ ROIs]. Each of these correlation values was transformed into a Z score using Fisher's $r-Z$ transformation. For each of the ROI pairs, group level statistics were performed to compare differences in connectivity strength between the groups (Fig. 2).

Group level statistics comparing HCs and WC patients at run 1 were calculated using a two-sample t test. Group level comparison of R1 and R2 in WC patients was performed using a paired t test.

For each of the ROI pairs that displayed group level differences in connectivity strength between the HCs and WC R1 and between WC R1 and WC R2, raw Pearson correlation values were extracted for WC subjects before and after the rTMS. Each of these connectivity strengths at R1 and R2 were correlated

Table 2 List of seeds selected for the analysis with their *x*, *y* and *z* coordinates as per the MNI template

X	Y	Z	Code	Area
32	−20	48	RPCG1	Right precentral gyrus
−32	−20	48	LPCG1	Left precentral gyrus
−12	−16	64	LSMA1	Left supplementary motor area
12	−16	64	RSMA1	Right supplementary motor area
−26	−48	−36	LCBM1	Left cerebellum
−36	−62	−34	LCBM2	Left cerebellum
14	−42	−20	RCBM3	Right cerebellum
24	−52	−30	RCBM4	Right cerebellum
0	50	−1	RMPF1	Right medial prefrontal
−10	−54	14	LPCC1	Left posterior cingulate
10	−54	14	RPCC1	Right posterior cingulate
−32	−16	66	LPCG2	Left precentral gyrus
−8	−4	64	LSMA2	Left supplementary motor area
2	2	46	RSMA2	Right supplementary motor area
−24	−40	68	POG1	Left post central gyrus
28	−36	70	RPOG1	Right post central gyrus
−8	−62	−10	LCBM3	Left cerebellum
−12	−20	8	LTHM1	Left thalamus
12	−20	8	RTHM1	Right thalamus
−22	−2	2	LPUT1	Left putamen
22	−2	2	RPUT1	Right putamen
−14	−4	−2	LMGP1	Left medial globus pallidus
14	−4	−2	RMGP1	Right medial globus pallidus
−48	−42	54	LIPS1	Left intraparietal sulcus
−34	−46	60	LSPC1	Left superior parietal cortex
−14	−54	64	LSPC2	Left superior parietal cortex
48	−42	54	RIPS1	Right intraparietal sulcus
34	−46	60	RSPC1	Right superior parietal cortex
14	−54	64	RSPC2	Right superior parietal cortex
−27	−49	−35	L-CBM	L-cerebellum
−12	−20	8	L-THM	L-thalamus
−22	−2	2	L-PUT	L-putamen
−12	−16	64	L-SMA	L-supplementary motor area
−14	−4	−2	L-MGP	L-medial globus pallidus
−48	−42	54	L-IPS	Left-inferior parietal sulcus
−32	−20	48	L-PCG	L-precentral gyrus
−12	8	10	L-Caud	L-caudate
−9	50	−2	L-MFG	L-medial frontal gyrus
−30	−29	26	L-LFG	L-lateral frontal gyrus
−39	−7	10	L-INSULA	L-insula
−52	−39	0	L-TG	L-temporal gyrus
−9	32	7	L-ACC	L-anterior cingulate cortex
−38	17	5	L-FrOpp	L-frontal oppeculum
−36	−46	49	L-ParLobe	L-parietal lobe
−5	60	−15	L-OrFrnt	L-orbitofrontal gyrus
−20	5	0	L-GP	L-globus pallidus
−28	−36	70	L-POG	L-post central gyrus
−19	40	27	L-SFG	L-superior frontal gyrus
−9	−32	−48	B-Stem	Brain stem
27	−49	−35	R-CBM	R-cerebellum
12	−20	8	R-THM	R-thalamus
22	−2	2	R-PUT	R-putamen
12	−16	64	R-SMA	R-supplementary motor area
14	−4	−2	R-MGP	R-medial globus pallidus
48	−42	54	R-IPS	R-inferior parietal sulcus
32	−20	48	R-PCG	R-precentral gyrus
12	8	10	R-Caud	R-caudate
9	50	−2	R-MFG	R-medial frontal gyrus
30	−29	26	R-LFG	R-lateral frontal gyrus
39	−7	10	R-Insula	R-insula
52	39	0	R-TG	R-temporal gyrus
9	32	7	R-ACC	R-anterior cingulate cortex
38	17	5	R-FrOpp	R-frontal oppeculum
36	−46	49	R-ParLobe	R-parietal lobe
5	60	−15	R-OrFrnt	R-orbitofrontal gyrus
20	5	0	R-GP	R-globus pallidus
28	−36	70	R-POG	R-post central gyrus
19	40	27	R-SFG	R-superior frontal gyrus
−44	−24	2	IFG	Inferior frontal gyrus
10	−54	14	PCC	Posterior cingulate cortex

with disease duration to assess whether rTMS can affect connectivity strengths in patients with longer disease duration.

Results

Because head motion is a concern in most fMRI studies, especially resting state studies [34,35], all the data from each of the subjects were tested for the presence of any head motion. Motion correction was performed using SPM8. During the motion analysis, two subjects from both the groups were excluded because they had more than 1.5 mm (maximum frame-wise displacement) movement during the study. Hence for all the subsequent analysis only 17 WC and 18 HC subjects were used. For each of the subjects, mean frame-wise displacement was calculated. Group level statistics were performed comparing the mean frame-wise displacement between the three subject groups to assess whether the groups differed in motion characteristics. No significant group level difference in head motion was observed between the HCs and WC R1 ($P = 0.7924$) and between WC R1 and WC R2 ($P = 0.2685$). As there were no group level differences observed in mean motion between the groups, mean motion was not included as a covariate in subsequent group level analysis.

The WC patients had a significant decrease in RSFC compared with HCs involving the left cerebellum, bilateral thalamus, bilateral putamen, bilateral globus pallidus, bilateral SMA, left intraparietal sulcus and left premotor cortex [$P < 0.05$, family-wise error (FWE) corrected]. Data obtained in WC subjects immediately following rTMS significantly modulated these networks by increasing the strength of the connections by predominantly modifying the left cerebellum, bilateral basal ganglia and left parietal cortex connections.

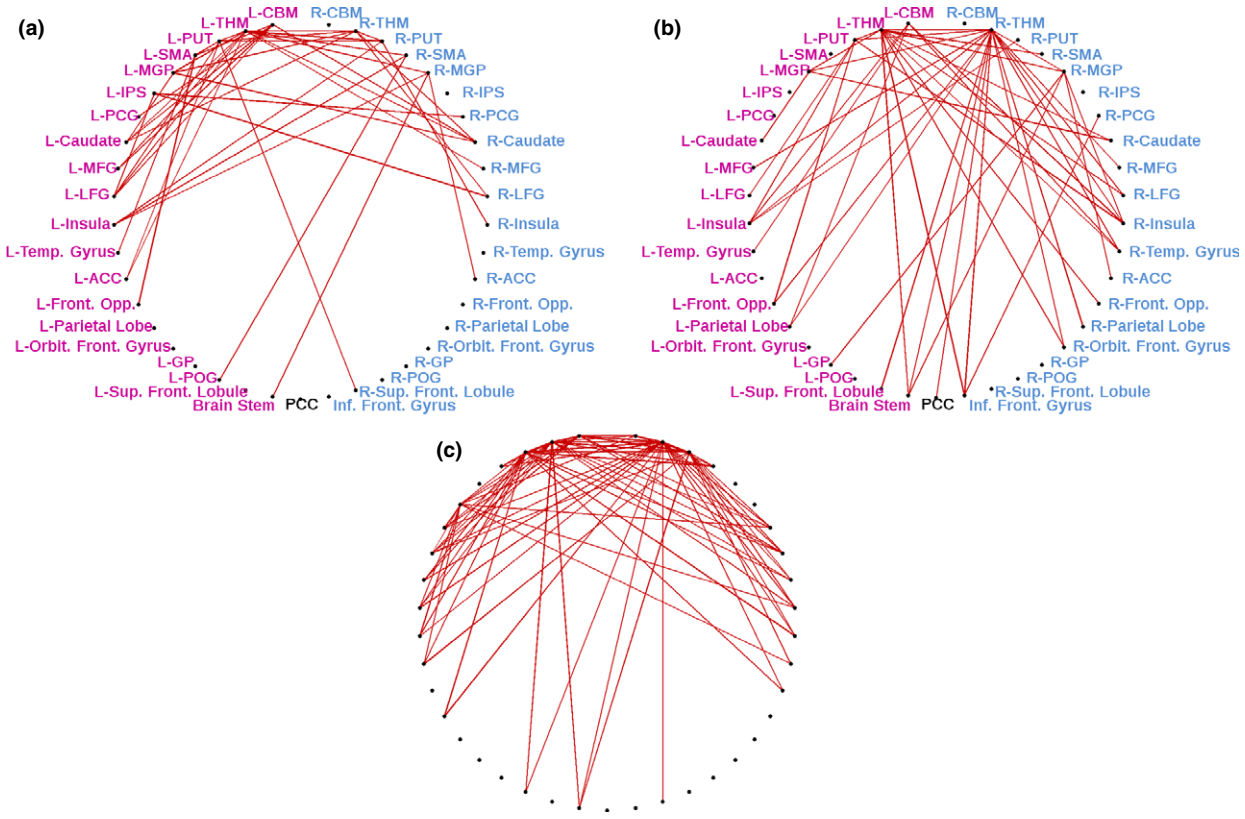

Figure 1 Illustrative representation of the network topology of the motor network. The lines represent the connections between the source seed region and the target seed region. These results demonstrate the baseline connectivity of various subcomponents of motor cortex in patients with writer's cramp (a) prior to repetitive transcranial magnetic stimulation ($P < 0.05$, family-wise error corrected). Reduced connectivity of all the seeds can be observed in comparison with the healthy controls (c). (b) Connectivity after a single session of repetitive transcranial magnetic stimulation which demonstrates diffuse increased connections with aggregation involving the cerebellum and basal ganglia.

Figure 1 displays the topology of the RSFC of the motor network in HCs and WC patients. Significant differences in connectivity topology can be observed between HCs (Fig. 1c) and WC patients at R1 (Fig. 1a). Modulation of connectivity as an effect of rTMS session is also visible in WC patients (Fig. 1b).

Seed-based connectivity analysis

Disease-induced connectivity differences

Seed-based connectivity analysis revealed that WC patients had overall reduced connectivity in all the evaluated regions of the motor network compared to HCs ($P < 0.05$, FWE correction). The regions which showed significant ($P < 0.05$, FWE corrected) reduction in connectivity were the left cerebellum, bilateral thalamus, bilateral putamen, bilateral globus pallidus, bilateral SMA, left intraparietal sulcus and left premotor cortex. Bilateral post central gyrus, right intraparietal sulcus, bilateral superior parietal cortex, the right medial prefrontal lobe, right premotor cortex and bilateral posterior cingulate cortex did not show any significant RSFC changes in comparison with HCs.

Repetitive transcranial magnetic stimulation induced connectivity differences

It was found that rTMS induced an increase in the connectivity in all seeds of the motor network that were evaluated. None of the regions showed decreased connectivity in R2 compared to R1. The regions which showed significant ($P < 0.05$, FWE corrected) increase in connectivity were the left cerebellum, bilateral thalamus, bilateral putamen, left intraparietal sulcus and left superior parietal cortex. No significant modulation was shown by both the globi pallidi, the bilateral SMA, left premotor cortex, bilateral post central gyrus, right intraparietal sulcus, bilateral superior parietal cortex, the right medial prefrontal lobe, right premotor cortex and bilateral posterior cingulate cortex.

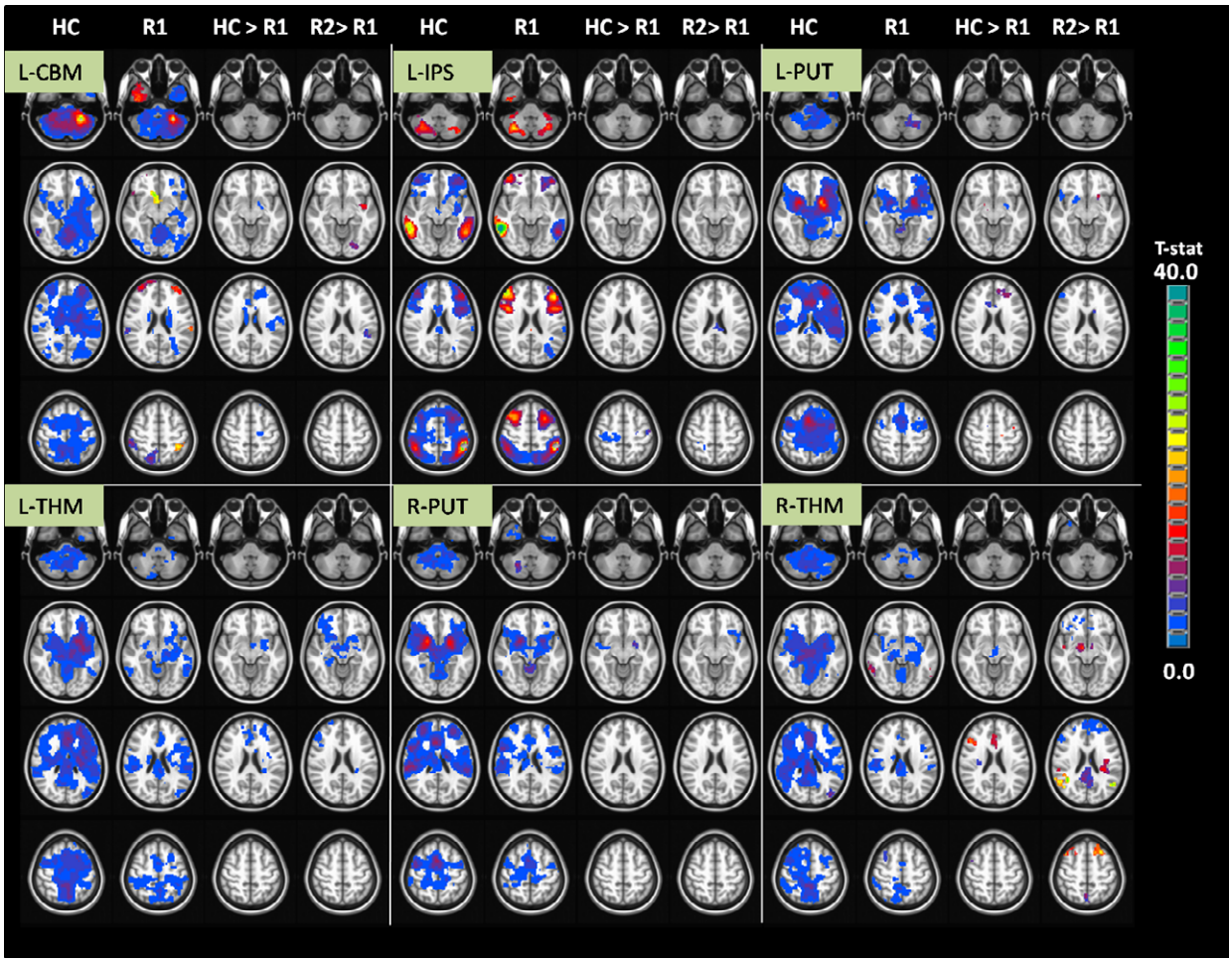

Figure 2 Composite image of the mean seed-based correlation maps in six different seeds, namely the left cerebellum (L-CBM), left intraparietal sulcus (L-IPS), left putamen (L-PUT), left thalamus (L-THM), right putamen (R-PUT) and right thalamus (R-THM); mean *t* statistic seed-based correlations of the significant areas are presented in the warm colours. Each section has four rows at four different axial levels, namely the cerebellum, mid brain, ventricles and supraventricular sections. The columns in each section represent various contrasts, namely mean image of healthy control (HCs), Pre rTMS (R1), HC > Pre rTMS (R1) and Post rTMS (R2) > Pre rTMS (R1) respectively.

Figure 2 represents the seed-based connectivity analysis of the various ROIs which were found to be significantly different between the groups.

Group level correlation analysis

A group level correlation matrix showing the pairwise correlation coefficient between each seed region with every other seed region is shown in Fig. 3. Figure 3a compares the pairwise correlation coefficient for each of the ROI pairs between HCs and R1. The lower diagonal matrix represents the HC group, whilst the upper diagonal matrix represents the R1 group. ROI pairs that showed significant differences in connectivity strength between the two groups have been marked with a circle. Group level analysis of HCs versus R1 ($P < 0.01$, FWE corrected) revealed that the left cerebellum, left thalamus, left globus pallidus, left putamen, bilateral SMA, right medial prefrontal lobe and right post central gyrus were significantly underconnected in WC patients in comparison with HCs. Group level analysis of R2 versus R1 ($P < 0.01$, FWE corrected) revealed that connectivity between the left thalamus, right globus pallidus, right thalamus and right prefrontal lobe were significantly modulated immediately following rTMS. Figure 3 represents the group level statistics of all the ROI-based connectivity differences for all the group level comparisons (HC−R1 and R2−R1).

Correlation with disease duration

Amongst the 17 subjects with WC, 14 subjects had disease duration <3 years and only three subjects had

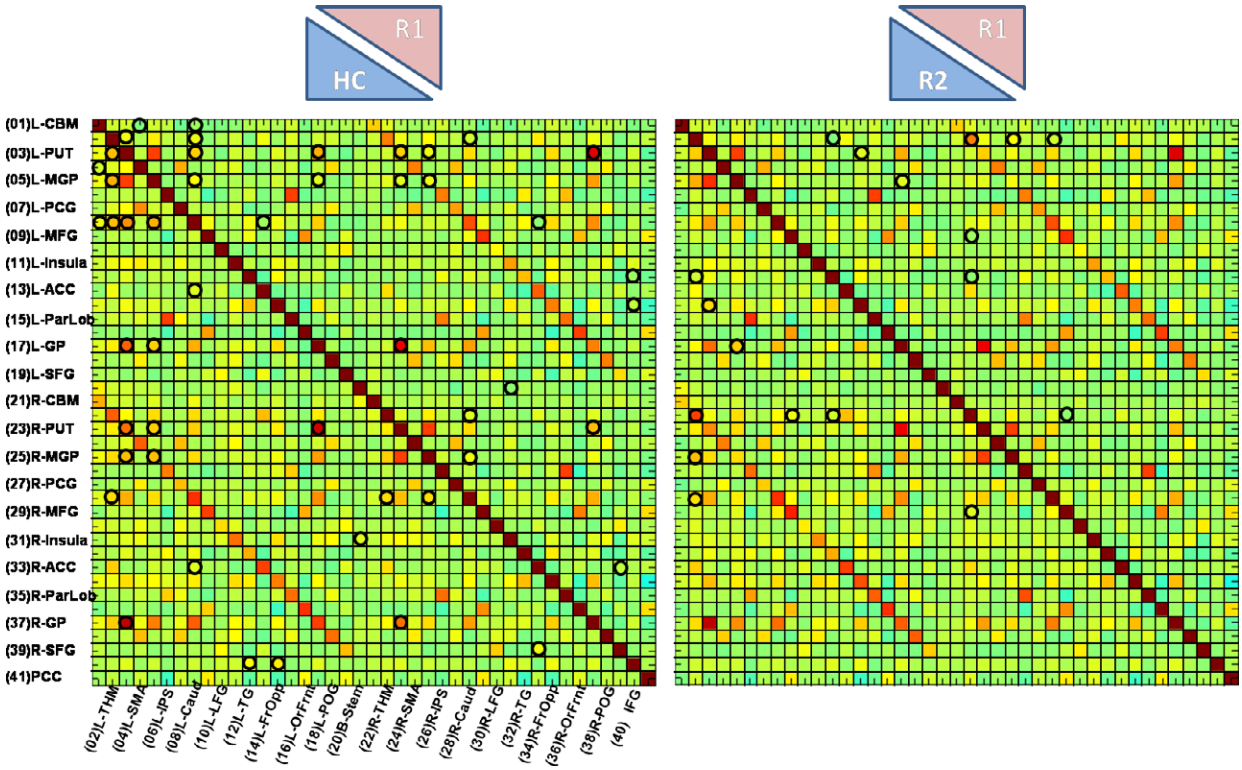

Figure 3 A group level correlation matrix showing the pairwise correlation coefficient between each of the seed regions with every other seed region is shown. (a) Pairwise correlation coefficient between HC and R1. The lower diagonal matrix represents the HC group, whilst the upper diagonal matrix represents the R1 group (Pairwise regions with significant differences between the two groups have been marked with a circle). (b) Pairwise correlation coefficient between R2 and R1. The lower diagonal represents R2 and upper diagonal represents R1.

duration more than 10 years. A trend towards significance was noted within several regions and is presented in Fig. 4. However, no significant functional connectivity correlating with disease duration was found.

Amongst the nine regions studied, six regions had negative correlation with reduction in connectivity as the duration of disease increased and three had positive correlation with increased connectivity with disease duration. The connectivity of the lateral globus pallidus, bilateral putamen and bilateral SMA was negatively correlated with disease duration. The positively correlated ROIs were the left cerebellum, left medial globus pallidus and left putamen. When an evaluation was done of whether rTMS-induced RSFC changes were dependent on duration of disease it was again found that the rTMS-induced increased connectivity was limited to connections of the left cerebellum. Figure 4 represents the disease correlations of the various networks which were found significant.

Discussion

It is surprising that a few decades ago dystonia was considered as a psychiatric disorder and now it is being increasingly accepted as a neurological functional network disorder based on various clinical and imaging studies [36]. rTMS is a valid tool used in modulating the network non-invasively and is increasingly used as a therapeutic tool [37] with varying degrees of clinical response. The utility of rTMS as a therapeutic modality in focal hand dystonias has been explored previously by Havrankova *et al.* [29] and Borich *et al.* [38] who have demonstrated improved writing after 1 Hz rTMS on somatosensory cortex and premotor cortex respectively. RSFC analysis is capable of visualizing the whole brain function and thus not only helps in understanding the pathophysiology of idiopathic disorders such as WC but also helps in non-invasively probing the plasticity induced by rTMS. Visualization of these abnormalities if applicable in a single patient could assist in clinical diagnosis, as more often than not structural imaging is normal in WC. Visualization and quantification of rTMS-induced modulations non-invasively could potentially help in selecting patients who would benefit from such therapy.

In our study it was found that patients with WC had widespread reduced connectivity involving the

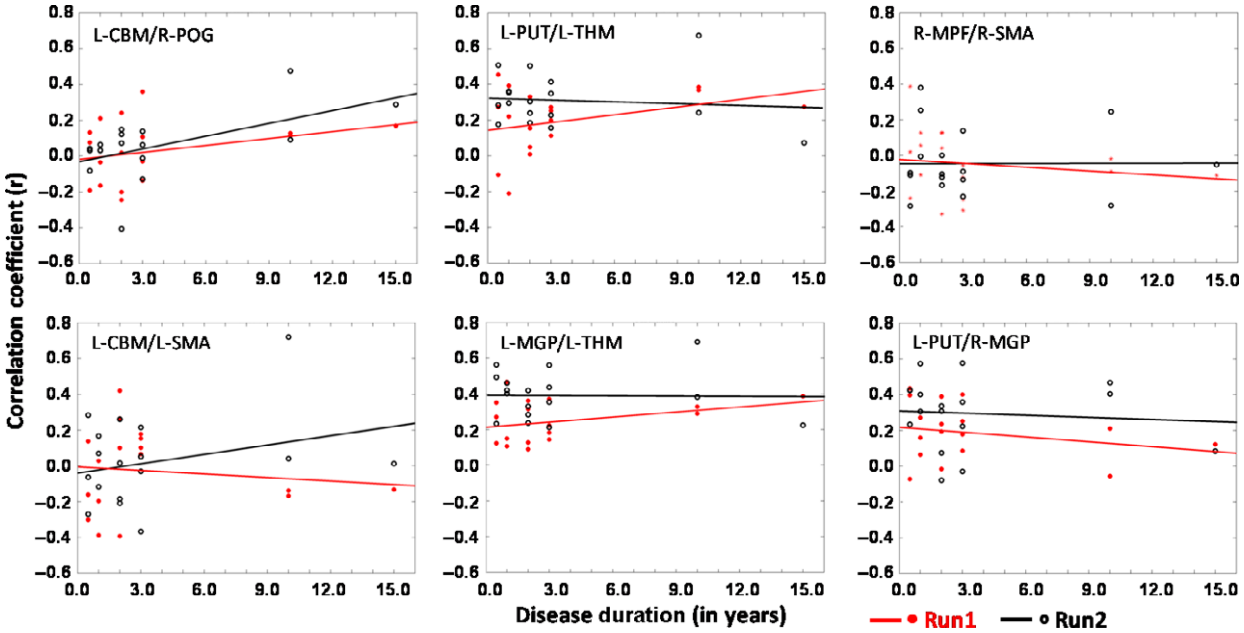

Figure 4 Scatter plots for disease duration in years compared with resting state functional connectivity strength between different seeds presented as a black line representing R2 and a red line representing R1. The connections of the left cerebellum, left putamen and left medial globus pallidus show a trend towards a positive correlation demonstrated as an upward slanting red line. The left cerebellum seed is noted to have positive modulation with repetitive transcranial magnetic stimulation seen as an upward slanting black line. The rest of the seeds do not show any significant modulations due to repetitive transcranial magnetic stimulation.

cerebellum, thalamus, globus pallidus and putamen on the left side, bilateral SMA, right medial prefrontal lobe and right post central gyrus in comparison with age matched controls. Our observations are similar to those reported by several previous studies [30,31,33]. However, unlike other studies the involvement in our study is widespread because several additional ROIs were used in the entire motor network and not only the premotor and sensory motor cortex. Although seed-based connectivity analysis revealed a decrease in connectivity of the left intraparietal region with bilateral premotor and right precentral gyrus in WC similar to that reported earlier, group level correlation analysis did not find significance in these areas. The reasons for differences in observations in the areas which are affected could be multifactorial and could include patient related factors such as disease duration and severity, methodological differences such as coordinate selection for definition of the ROI, the level of statistical significance etc.; a trend towards decreased connectivity in the bilateral globus pallidus, putamen and SMA with disease duration was also found, similar to the findings of Delnooz *et al*. [30]. The novel finding of a trend towards increasing connectivity of the left cerebellum, left putamen and globus pallidum with disease duration is very interesting as it signifies that these areas are developing increasing connections perhaps as a compensatory phenomenon as the disease progressed.

A single session of rTMS induced widespread increase in connectivity significantly involving basal ganglia networks. The network that was significantly altered after rTMS was the left thalamus–right globus pallidus–right thalamus and right prefrontal lobe. Additionally the areas connected with the left cerebellum had a trend towards increasing connections after rTMS. A single session of rTMS did not induce any significant changes in the connections of the left premotor cortex and supplementary cortex contrary to our expectations based on previous studies using rTMS. Since all the patients in our study had only right side symptoms it could be possible that the disease-induced decreased connectivity affected the left motor network more severely and hence a single session of rTMS could not make any further changes in these networks. It is also possible that this was because these areas were subjacent to the rTMS site and hence had decreased BOLD response immediately after the rTMS. Based on the finding of a positive correlation of cerebellar connectivity with disease duration and the evidence that only its connections showed significant modulation after rTMS, it is proposed that changes induced by a single session of rTMS probably work through preserved connections.

This finding is also supported by the fact that the majority of changes after rTMS were in the contralateral hemisphere, namely the right globus pallidus, right thalamus and right prefrontal lobe where the connections would have been relatively preserved since all our patients had only right-handed symptoms. This finding is unique to our study; however, it needs to be noted that EEG functional connectivity measures [27] have also shown modulations of inter-hemispheric and interregional connections after successful rTMS therapy which could be supportive of our findings.

In this study networks other than the motor network were not evaluated and also a ROI correlation with other brain regions not considered in the parcellation was not assessed. Since there are increasing reports of non-motor manifestations in patients with dystonia [34] it is possible that other networks are also involved. Future studies could look into assessing these using physiological methods for analysis. It is also seen that right-hand-affected patients also develop left-hand dystonia after they initiate left-handed writing. Since only right-handed and right-affected WC patients were evaluated, underlying functional connectivity abnormalities in cases of left-sided WC symptoms and left-handed patients remain unexplored. The long-term plasticity changes induced by therapeutic rTMS (daily sessions for 7–10 days) which could have had direct clinical application were not evaluated. It is possible that the changes observed are transient and could vary with time as the changes were not evaluated serially. Since the number of subjects was low the correlation with disease duration and severity had no statistical significance. Another factor is that resting state activity is not sufficiently controlled and does not address the task-related changes in movement strategies or functional compensation that occur only during motor performance; hence task-based connectivity analysis in addition would have made the evaluation more complete.

Conclusions

Resting state functional connectivity analysis in patients with WC reveals decreased connectivity involving several areas of the motor network. The changes induced by a single session of rTMS are diffuse and involve subcortical structures, are trans-hemispheric and probably act through areas showing preserved connections such as the cerebellum. Hence it is concluded that WC is a network disorder with widespread dysfunction much larger than clinically evident and RSFC analysis is a viable non-invasive tool for probing its pathophysiology and plasticity.

Acknowledgements

We acknowledge the support of the Department of Science and Technology, Government of India, for providing the 3 T MRI scanner exclusively for research in the field of neurosciences. We are extremely grateful to Dr Shobini L. Rao (Department of Clinical Psychology, NIMHANS, India) for her untiring attitude and inspiration. We thank all the patients who participated in this study without expecting anything in return. We are grateful to the staff especially the radiographers (Department of Neuroimaging and Interventional Radiology, NIMHANS, India) for their odd hours support during data collection.

Disclosure of conflicts of interest

The authors declare no financial or other conflicts of interest.

References

1. Defazio G, Berardelli A, Hallett M. Do primary adult-onset focal dystonias share aetiological factors? *Brain* 2007; **130:** 1183–1193.
2. Hallett M. Pathophysiology of writer's cramp. *Hum Mov Sci* 2006; **25:** 454–463.
3. Quartarone A, Hallett M. Emerging concepts in the physiological basis of dystonia. *Mov Disord* 2013; **28:** 958–967.
4. Hallett M. Neurophysiology of dystonia: the role of inhibition. *Neurobiol Dis* 2011; **42:** 177–184.
5. Perlmutter JS, Mink JW. Dysfunction of dopaminergic pathways in dystonia. *Adv Neurol* 2004; **94:** 163.
6. Segawa M. Dopa-responsive dystonia. *Handb Clin Neurol* 2010; **100:** 539–557.
7. Tabbal S, Mink J, Antenor J, Carl J, Moerlein S, Perlmutter J. 1-Methyl-4-phenyl-1,2,3,6-tetrahydropyridine-induced acute transient dystonia in monkeys associated with low striatal dopamine. *Neuroscience* 2006; **141:** 1281–1287.
8. Levy LM, Hallett M. Impaired brain GABA in focal dystonia. *Ann Neurol* 2002; **51:** 93–101.
9. Candia V, Elbert T, Altenmüller E, Rau H, Schäfer T, Taub E. Constraint-induced movement therapy for focal hand dystonia in musicians. *Lancet* 1999; **353:** 42.
10. Byl NN, Archer ES, McKenzie A. Focal hand dystonia: effectiveness of a home program of fitness and learning-based sensorimotor and memory training. *J Hand Ther* 2009; **22:** 183–198.
11. Delnooz C, Helmich RC, Medendorp W, Van de Warrenburg BP, Toni I. Writer's cramp: increased dorsal premotor activity during intended writing. *Hum Brain Mapp* 2013; **34:** 613–625.
12. Castrop F, Dresel C, Hennenlotter A, Zimmer C, Haslinger B. Basal ganglia–premotor dysfunction during movement imagination in writer's cramp. *Mov Disord* 2012; **27:** 1432–1439.
13. de Vries PM, Johnson KA, de Jong BM, *et al*. Changed patterns of cerebral activation related to clinically normal hand movement in cervical dystonia. *Clin Neurol Neurosurg* 2008; **110:** 120–128.
14. Huang YZ, Rothwell JC, Lu CS, Wang J, Chen RS. Restoration of motor inhibition through an abnormal premotor–motor connection in dystonia. *Mov Disord* 2010; **25:** 696–703.
15. Islam T, Kupsch A, Bruhn H, Scheurig C, Schmidt S, Hoffmann K-T. Decreased bilateral cortical representation patterns in writer's cramp: a functional magnetic resonance imaging study at 3.0 T. *Neurol Sci* 2009; **30:** 219–226.
16. Preibisch C, Berg D, Hofmann E, Solymosi L, Naumann M. Cerebral activation patterns in patients with writer's cramp: a functional magnetic resonance imaging study. *J Neurol* 2001; **248:** 10–17.
17. Nelson AJ, Blake DT, Chen R. Digit-specific aberrations in the primary somatosensory cortex in writer's cramp. *Ann Neurol* 2009; **66:** 146–154.
18. Meunier S, Garnero L, Ducorps A, *et al*. Human brain mapping in dystonia reveals both endophenotypic traits and adaptive reorganization. *Ann Neurol* 2001; **50:** 521–527.
19. Delmaire C, Vidailhet M, Elbaz A, *et al*. Structural abnormalities in the cerebellum and sensorimotor circuit in writer's cramp. *Neurology* 2007; **69:** 376–380.
20. Delmaire C, Vidailhet M, Wassermann D, *et al*. Diffusion abnormalities in the primary sensorimotor pathways in writer's cramp. *Arch Neurol* 2009; **66:** 502–508.
21. Vitek JL, Chockkan V, Zhang JY, *et al*. Neuronal activity in the basal ganglia in patients with generalized dystonia and hemiballismus. *Ann Neurol* 1999; **46:** 22–35.
22. Chen R, Wassermann EM, Caños M, Hallett M. Impaired inhibition in writer's cramp during voluntary muscle activation. *Neurology* 1997; **49:** 1054–1059.
23. Münchau A, Schrag A, Chuang C, *et al*. Arm tremor in cervical dystonia differs from essential tremor and can be classified by onset age and spread of symptoms. *Brain* 2001; **124:** 1765–1776.
24. Blood AJ. Imaging studies in focal dystonias: a systems level approach to studying a systems level disorder. *Curr Neuropharmacol* 2013; **11:** 3.
25. Ilmoniemi RJ, Virtanen J, Ruohonen J, Karhu J, Aronen HJ, Katila T. Neuronal responses to magnetic stimulation reveal cortical reactivity and connectivity. *Neuroreport* 1997; **8:** 3537–3540.
26. Komssi S, Aronen HJ, Huttunen J, *et al*. Ipsi- and contralateral EEG reactions to transcranial magnetic stimulation. *Clin Neurophysiol* 2002; **113:** 175–184.
27. Shafi MM, Westover MB, Oberman L, Cash SS, Pascual-Leone A. Modulation of EEG functional connectivity networks in subjects undergoing repetitive transcranial magnetic stimulation. *Brain Topogr* 2014; **27:** 172–191.
28. Schneider SA, Pleger B, Draganski B, *et al*. Modulatory effects of 5 Hz rTMS over the primary somatosensory cortex in focal dystonia – an fMRI-TMS study. *Mov Disord* 2010; **25:** 76–83.
29. Havrankova P, Jech R, Walker ND, *et al*. Repetitive TMS of the somatosensory cortex improves writer's cramp and enhances cortical activity. *Neuro Endocrinol Lett* 2010; **31:** 73–86.
30. Delnooz C, Helmich RC, Toni I, van de Warrenburg BP. Reduced parietal connectivity with a premotor writing area in writer's cramp. *Mov Disord* 2012; **27:** 1425–1431.
31. Dresel C, Haslinger B, Castrop F, Wohlschlaeger AM, Ceballos-Baumann AO. Silent event-related fMRI reveals deficient motor and enhanced somatosensory activation in orofacial dystonia. *Brain* 2006; **129:** 36–46.
32. Hinkley LB, Webster RL, Byl NN, Nagarajan SS. Neuroimaging characteristics of patients with focal hand dystonia. *J Hand Ther* 2009; **22:** 125–135.
33. Mohammadi B, Kollewe K, Samii A, Beckmann CF, Dengler R, Münte TF. Changes in resting-state brain networks in writer's cramp. *Hum Brain Mapp* 2012; **33:** 840–848.
34. Stamelou M, Edwards MJ, Hallett M, Bhatia KP. The non-motor syndrome of primary dystonia: clinical and pathophysiological implications. *Brain* 2012; **135:** 1668–1681.
35. Van Dijk KR, Sabuncu MR, Buckner RL. The influence of head motion on intrinsic functional connectivity MRI. *NeuroImage* 2012; **59:** 431–438.
36. Torres-Russotto D, Perlmutter JS. Task-specific dystonias. *Ann NY Acad Sci* 2008; **1142:** 179–199.

37. Pleger B, Blankenburg F, Bestmann S, *et al*. Repetitive transcranial magnetic stimulation-induced changes in sensorimotor coupling parallel improvements of somatosensation in humans. *J Neurosci* 2006; **26:** 1945–1952.

38. Borich M, Arora S, Kimberley TJ. Lasting effects of repeated rTMS application in focal hand dystonia. *Restor Neurol Neurosci* 2009; **27:** 55–65.